Acta of Bioengineering and Biomechanics
Vol. 20, No. 3, 2018

Original paper
DOI: 10.5277/ABB-01143-2018-03

A simple method of incorporating the effect of the Uniform Stress Hypothesis in arterial wall stress computations

GRAND ROMAN JOLDES[1], CHRISTOPHER NOBLE[2], STANISLAV POLZER[3], ZEIKE A TAYLOR[2], ADAM WITTEK[1], KAROL MILLER[1, 4]*

[1] Intelligent Systems for Medicine Laboratory, The University of Western Australia, Perth Australia.
[2] Centre for Computational Imaging and Simulation Technologies in Biomedicine, Institute for in silico Medicine, Department of Mechanical Engineering, The University of Sheffield, Sheffield, UK.
[3] Department of Applied Mechanics, VSB-Technical University Ostrava, Ostrava, Czech Republic.
[4] School of Engineering, Cardiff University, Cardiff, UK.

Purpose: Residual stress has a great influence on the mechanical behaviour of arterial wall. Numerous research groups used the Uniform Stress Hypothesis to allow the inclusion of the effects of residual stress when computing stress distributions in the arterial wall. Nevertheless, the available methods used for this purpose are very expensive, due to their iterative nature. In this paper we present a new method for including the effects of residual stress on the computed stress distribution in the arterial wall. *Methods*: The new method using the Uniform Stress Hypothesis enables computing the effect of residual stress by averaging stresses across the thickness of the arterial wall. *Results*: Being a post-processing method for the computed stress distributions, the proposed method is computationally inexpensive and, thus, better suited for clinical applications than the previously used ones. *Conclusions*: The resulting stress distributions and values obtained using the proposed method based on the Uniform Stress Hypothesis are very close to the ones returned by an existing iterative method.

Key words: *Uniform Stress Hypothesis, residual stress, finite element method, arterial wall stress*

1. Introduction

In this paper, an efficient method to include the effects of Residual Stress (RS) in patient specific arterial wall stress calculations was presented. Arterial wall stress calculations based on patient specific biomechanics have been proposed by many researchers, for applications such as rupture risk analysis in aortic abdominal aneurisms (AAA). Biomechanics-derived criteria, such as Peak Wall Stress, may constitute accurate predictors of arterial wall rupture [1], [2]. The potential value of such biomechanics-based approaches was explored in a recent review [3].

RS in arterial walls and its effect on the biomechanical response have been well documented [4]–[7]. Its importance with respect to the accurate stress computation is correspondingly clear. The significant circumferential component of RS in many vessels was demonstrated, for example, in opening angle tests [8].

Various approaches to incorporating RS into finite element simulations have been proposed. Raghavan et al. [9] used opening angle measurements by creating FE models of idealised and real arteries in "opened" (cut) configurations, then computing the wall stresses that result from closing the samples into rings Balzam et al. [10] used a similar open-to-closed ring simulation approach and transferred the resulting nodal

* Corresponding author: The University of Western Australia, Intelligent Systems for Medicine Laboratory, 35 Stirling Highway, 6009 Crawley, Australia. Phone: + 61 8 6488 8545, e-mail: karol.miller@uwa.edu.au
Received: May 10th, 2018
Accepted for publication: August 6th, 2018

coordinates and deformation gradient into a subsequent simulation step involving physiological loads. There is evidence in the literature that the RS may vary between the different arterial wall layers [8], and that a longitudinal pre-stress is also present [11]. Nevertheless, such information is of limited use in patient-specific stress computations, as these parameters vary greatly between individuals [11] and cannot be determined using non-invasive techniques.

In order to assess wall stress in patients, *non-invasive* estimation of RS is required, and techniques like opening angle tests are clearly excluded. Ambrosi et al. [12] have developed an axisymmetric analytical model of arteries with RS incorporated through a growth tensor based on thermodynamical arguments. Polzer et al. [13] proposed an algorithm for patient-specific RS estimation based on the assumption that remodelling-derived RS results in an even stress distribution across the vessel wall, according to the Uniform Stress Hypothesis (USH). Their algorithm estimates residual strains iteratively for patient-specific artery at given times, using a staggered two-field solution approach based on the concept of isotropic volumetric growth. More recently, a different staggered method was proposed [14]. Here by the USH was again assumed, but rather than by residual strains, the RS was estimated iteratively by updating a RS tensor in the loaded configuration.

Fig. 1. Depiction of the vessel wall without and with RS, according to the uniform stress hypothesis. The grayscale intensity reflects the stress magnitude, with lighter shades corresponding to lower stresses

In the present work, we propose a new method for incorporating the effects of RS (based on the USH), that is considerably less computationally-costly, but with accuracy similar to the method of Polzer et al. [13]. Given the stress distribution they found for a cylindrical artery, we assume that the RS acts to evenly distribute bending stresses across the arterial wall thickness (Fig. 1). We do not attempt to compute the RS itself, but instead modify the wall stress field so as to reflect the presence of RS on the arterial wall stress distribution. Combined with recently reported efficient techniques for estimating wall stress [15], [16], the proposed approach achieves fast solution and requires only standard clinical data as inputs (Computer Tomography-Angiography and blood pressure measurements).

2. Materials and methods

2.1. Hypothesis regarding influence of residual stress on the stress distribution in the arterial wall

The uniform stress hypothesis (USH) states that vascular tissue remodels itself toward a preferred stress-strain state, which, in turn, leads to homogenization of stress components across the wall [17]. An experimental study that supports the USH is that of Lu et al. [18], who introduced a unit step change in blood flow in rat femoral arteries to investigate the effect on wall remodeling. They found that greater growth in the vessel outer wall compared to in the inner wall resulted in a decrease in wall opening angle, which is consistent with non-uniform remodeling in the USH.

2.2. Model creation

The present study used anonymized data from seven patients that underwent Computer Tomography-Angiography (CT-A) of the aorta at St. Anne's University Hospital, Brno, Czech Republic, at an in-plane resolution of 0.5 mm and a slice thickness of 3 mm. Deformable (active) contour models (A4research vers.4.0, VASCOPS GmbH, Austria) were used to reconstruct the 3D geometry of AAAs from CT data [19]. After aneurysm segmentation, Stereo Lithography (STL) files representing the AAA's geometry (luminal surface, exterior surface, and wall-ILT interface) were exported to ICEM CFD (Ansys Inc., US) for FE mesh generation. The aneurysm wall was meshed with tri-linear hexahedral elements (element type SOLID 185, surface element size of 3 mm, four elements across the thickness) while the ILT was meshed with linear tetrahedral elements (element type SOLID 285, element size of 3 mm). The wall thickness was assumed homogeneous with a thickness of 2 mm. Mesh generation required significant manual interaction and took four to eight hours for each case. Sectional views of the meshes are shown in Fig. 2 and their size is presented in Table 1.

Table 1. Size of the patient-specific meshes for the analysed cases

Case number	Mesh size		
	Nodes	Tetras (ILT)	Hexas (Wall)
1	112587	95187	17400
2	37098	44185	22064
3	29253	1680	21648
4	50200	55968	30444
5	39248	50607	22344
6	28883	32988	17024
7	30551	51922	15232

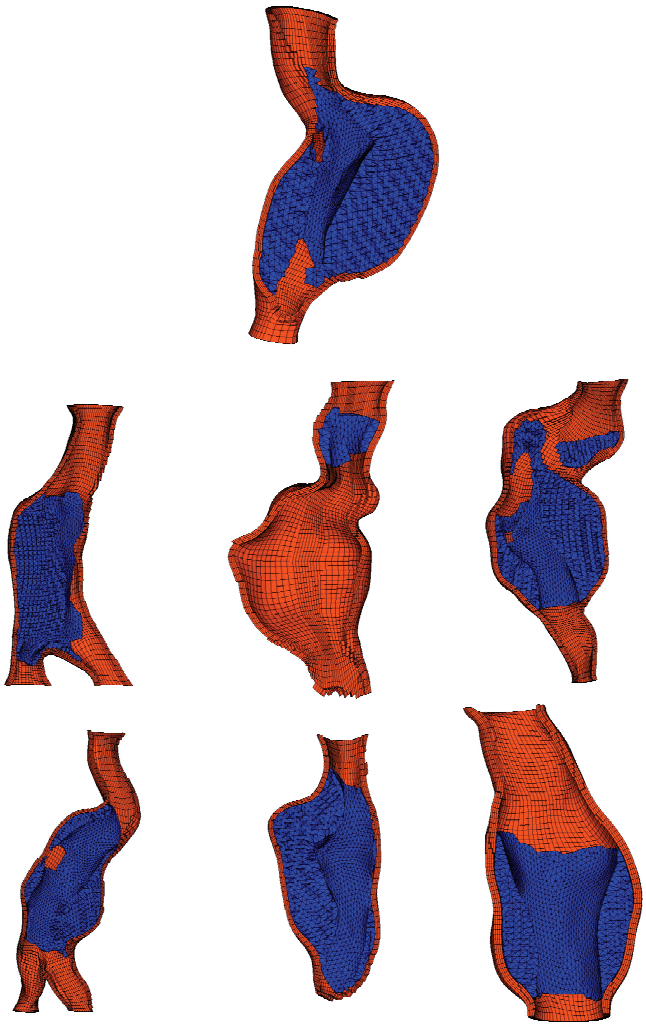

Fig. 2. Meshes generated for the 7 patient-specific models (red – AAA wall, blue – ILT)

Finite element meshes were exported to ANSYS 15.0 (Ansys Inc., US) for FE computation. Each AAA was fixed at renal arteries and below the aortic bifurcation. An ILT was considered to be ideally and permanently attached to aneurysmal wall, which was numerically ensured by using a bonded contact between the two volumes. We used a uniform incompressible fifth-order Yeoh strain energy density function to capture AAA wall mean population material properties [20]. The use of a complex geometry (such as AAAs) allows the testing of the proposed method under the most demanding circumstances.

2.3. Initial estimation of wall stress

The CT-A images record the aorta at pulsatile blood pressure, and therefore do not reflect AAA zero-pressure geometry, required for FE computation. A patient-specific mean arterial pressure (MAP = 1/3 systolic pressure + 2/3 diastolic pressure) was used to calculate the zero-pressure configuration using the backward incremental method [21], recently modified in [22]. Successive intermediate reference configurations were constructed by subtracting the computed FE-mesh nodal displacements from the previous reference configuration, i.e., until the pressure-loaded model matched the CT-A-recorded geometry within chosen tolerance. The stress distribution (without considering residual stress effects) was obtained as a consequence of computing the zero-pressure configuration.

2.4. Proposed new method of incorporating residual stress effects in the artery wall stress estimation

The proposed method aims to simplify the existing iterative approaches and replace them with a simple single-step calculation. Considering the wall cross-section shown in Fig. 1, in the absence of any RS, the stress along the wall thickness has two components: the hoop stress, created by the hoop forces, and the bending stress, generated by the bending moments. The average bending stress along the wall thickness is equal to zero (as it is created by moments). According to the USH, remodeling processes will impart a RS within the unloaded wall, so that, when loaded, the stresses are uniform across the wall thickness. At the same time, the equilibrium of forces must be satisfied, therefore, the internal wall forces created by this constant stress must be the same as the hoop forces obtained without the inclusion of RS (since with or without RS, the latter still reflect static equilibrium of the AAA with respect to the circulatory pressure loading):

$$\int_{R_1}^{R_2} \bar{\sigma}\mathbf{d}r = \int_{R_1}^{R_2} \sigma(r)\mathbf{d}r\,. \tag{1}$$

Therefore, to compute the constant stress $\overline{\sigma}$ according to the USH, the stresses σ found using the procedure in Section 2.3 (without considering RS) are averaged across the vessel wall according to

$$\overline{\sigma} = \frac{1}{T}\int_{R_1}^{R_2} \sigma(r)\mathbf{d}r\,, \tag{2}$$

where $T = R_2 - R_1$ is the wall thickness and $\sigma(r)$ is the stress component being averaged, which is a function of the radial coordinate r.

With more complicated 3D geometry, the above equations do not really apply. Nevertheless, under the assumption that the AAA wall is relatively thin, the hoop stress is the main stress occurring in the wall, which potentially is the one, responsible for the wall rupture. Therefore, we make the assumption that the principal stress directions have the same orientation across the thickness of the wall and apply Eq. (2) to the maximum principal stress (MPS) component to find the value of the maximum wall stress under the USH. The stresses are evaluated for each node of the external surface of the arterial wall discretization for the purpose of visualization and comparison to other methods.

To obtain an accurate value of the average stress, the integral term in (2) is computed as a sum of piecewise integrals evaluated on several smaller sub-intervals of the wall thickness, so

$$\overline{\sigma} = \frac{1}{T}\sum_{k=1}^{n}\int_{M_{k-1}}^{M_k} \sigma(r)\mathbf{d}r\,, \tag{3}$$

where M_k is the coordinate of the outer boundary of interval k (Fig. 3), and n is the number of sub-intervals. We use equal-sized sub-intervals, meaning their lengths are $\frac{T}{n}$, and boundary coordinates are given by:

$$M_k = \left(1 - \frac{k}{n}\right)R_1 + \frac{k}{n}R_2\,. \tag{4}$$

On each sub-interval, a two-point Gauss rule is employed, yielding:

$$\overline{\sigma} \approx \frac{1}{T}\sum_{k=1}^{n}\frac{M_k - M_{k-1}}{2}\sum_{i=1}^{2}\sigma_k^i = \frac{1}{2n}\sum_{k=1}^{n}\sum_{i=1}^{2}\sigma_k^i\,, \tag{5}$$

where σ_k^i is the stress value at Gauss point i within interval k. Gauss point coordinates in interval k are obtained with standard interval scaling formulae:

$$\begin{aligned} G_k^1 &= (1-s)M_{k-1} + sM_k \\ G_k^2 &= sM_{k-1} + (1-s)M_k \end{aligned} \tag{6}$$

with the position of the points controlled by:

$$s = \frac{1 - \sqrt{\frac{1}{3}}}{2}\,. \tag{7}$$

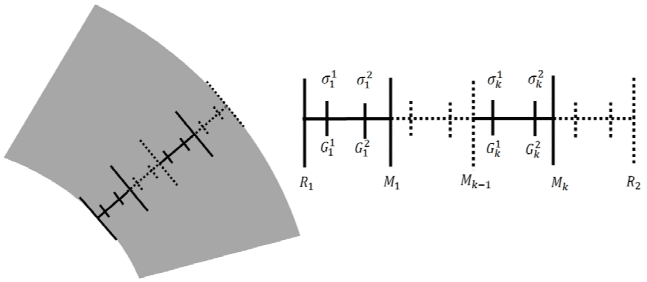

Fig. 3. Schematics detailing the Gauss integration procedure to calculate the average stress across the vessel wall. R_1 and R_2 represent inner and outer wall radii, respectively. Sub-interval k is bounded by coordinates M_{k-1} and M_k, and σ_k^1, σ_k^2 are the stresses evaluated at the Gauss points (G_k^1, G_k^2) of this sub-interval

To enable evaluation of the results of the proposed new algorithm, we first estimated RS for each case using the iterative and more computationally expensive algorithm proposed by [13]. The RS effect on both Peak Wall Stress (PWS – defined as maximum value of the maximum principal stress) and stress distribution were evaluated and the results from each method were compared.

3. Results

Stress distributions for seven AAA cases with and without the inclusion of RS effects were analyzed. The latter were included using both the existing method of Polzer et al. [13] and the newly proposed method In the new method, four sub-intervals across the wall thickness we used for accurate integration of stress. The stresses obtained from the FE analysis were extrapolated to the nodes of the mesh and then the stresses at the Gauss points used for stress integration across the wall were interpolated from these nodal values using algorithms from the Visualization Toolkit (VTK, available at www.vtk.org).

3.1. Assumption testing: MPS has the same direction across the thickness of the wall

During the derivation of the new method we assumed that the MPS has the same direction across the thickness of the wall. We tested this assumption by computing the MPS and its direction at all points of the mesh. We then studied the direction $\mathbf{D}^e$ of the MPS on the exterior arterial wall as well as the scalar product between $\mathbf{D}^e$ at a given point and the direction $\mathbf{D}^i$ of the MPS at the closest point on the interior arterial wall:

$$SP = |\mathbf{D}^e \cdot \mathbf{D}^i| \tag{8}$$

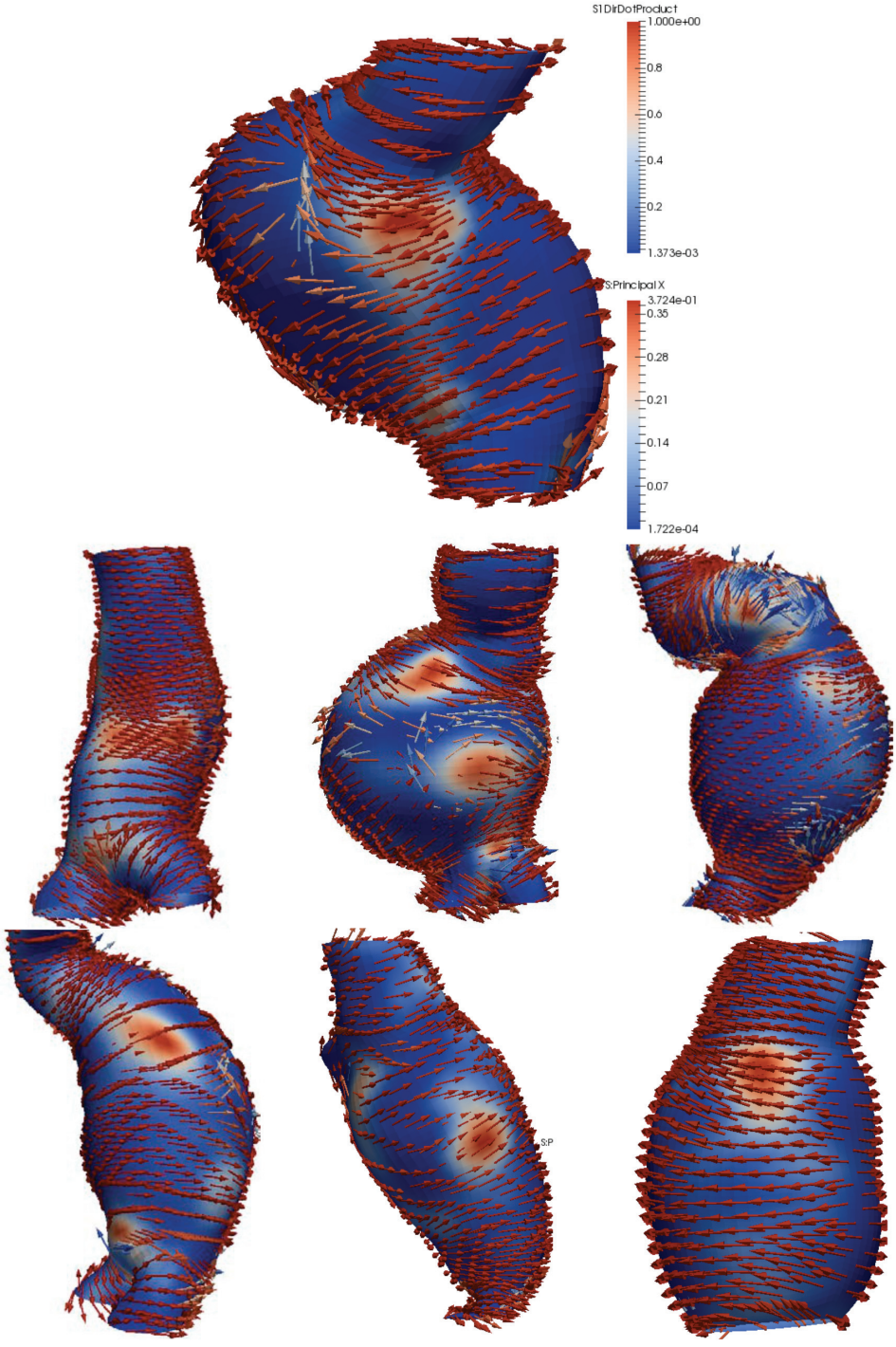

Fig. 4. Assumption test: MPS has the same direction across the thickness of the wall.
The arrows indicate the direction De of the MPS. The color of the arrows indicates the value of $|\mathbf{D}^e \cdot \mathbf{D}^i|$ (red = parallel directions).
The surface color indicates the value of the MPS (red = high stress)

This product has values of 1 or 0 if the two vectors are parallel or perpendicular, respectively.

The results, presented in Fig. 4, show that:

- The direction $\mathbf{D}^e$ of the MPS is tangent to the arterial wall, and, therefore, the MPS is the stress component responsible for wall rupture;
- On the most part of the arterial surface, the directions $\mathbf{D}^e$ and $\mathbf{D}^i$ are parallel, and, therefore, integrating the MPS across the wall thickness is expected to be accurate. The regions in which $\mathbf{D}^e$ and $\mathbf{D}^i$ are not parallel are not in areas of high stresses.

3.2. Evaluation of the new method

The effect of RS on the wall stress distribution computed using the existing method is shown in Fig. 5. This method reduces the differences in stress between the interior and exterior walls of the AAA, but does not create a completely uniform stress distribution across the wall thickness.

A comparison between the results obtained using the existing method and the proposed method for

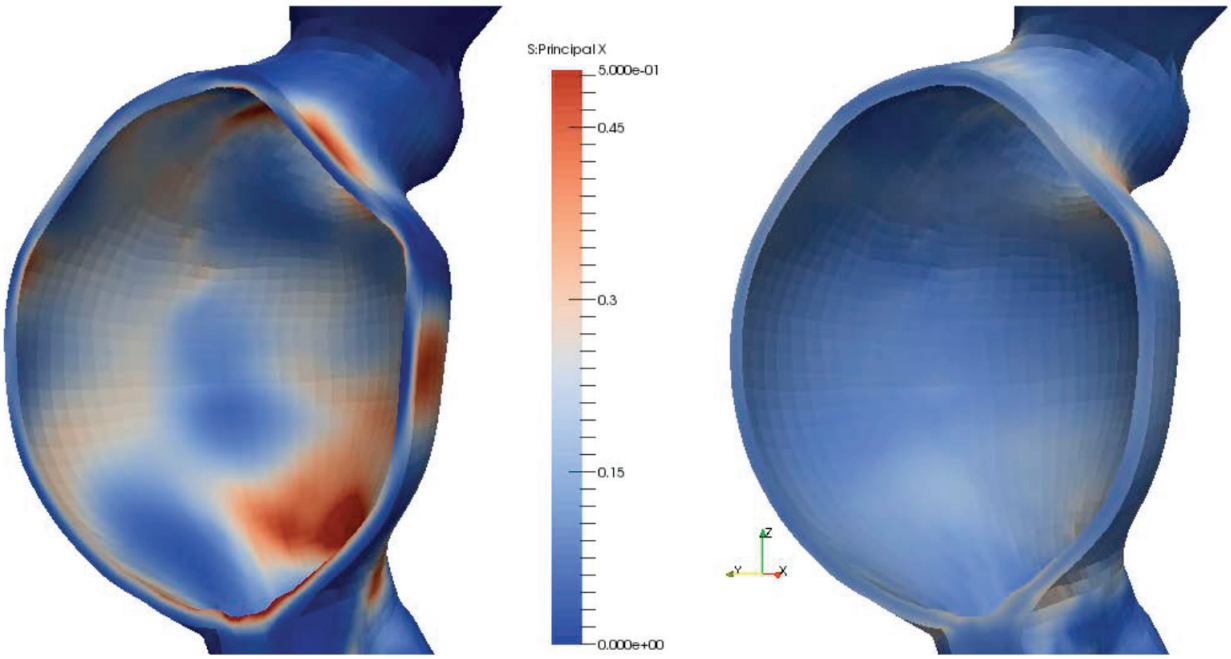

Fig. 5. The effect of inclusion of the residual stress in an AAA analysis: maximum principal stress distribution without (left) and with (right) residual stress included. The residual stress has been included using the existing method of Polzer et al. [13]. Intraluminal thrombus not shown

Table 2. Peak wall stress (PWS) values obtained using the new method for RS inclusion, the existing method for RS inclusion, and without RS inclusion

Case number	RS inclusion method		Difference [%]	No RS [MPa]
	New method [MPa]	Existing method [MPa]		
1	0.250	0.224	11.6	0.411
2	0.220	0.207	6.2	0.401
3	0.396	0.364	8.7	0.534
4	0.289	0.307	5.8	0.655
5	0.192	0.223	13.9	0.455
6	0.214	0.212	0.9	0.442
7	0.209	0.190	10	0.357

handling RS is presented in Fig. 6. The new method predicts very similar distributions and levels of stress. The differences in PWS were 8.2% on average, with a 4.2% standard deviation (Table 2). On most points on the arterial wall surface the stress differences are close to zero, as shown by the histograms in Fig. 6.

4. Discussion and conclusions

We developed a new method for including the effects of RS in FE analyses of arterial walls, based on the USH. The new method requires only the post-processing of a finite element analysis, making it very efficient computationally. To test the proposed method under the most demanding conditions, in our numerical experiments we used a highly non-linear material model, which produces large variations of stress across the wall thickness, and complex arterial geometry. The proposed method predicts similar stress distributions and values for the MPS as an existing iterative method, without the associated computational expense. Moreover, the predictions of PWS locations and magnitudes are similar between the two methods for all cases.

The comparative results obtained with and without the inclusion of RS highlight the influence of RS inclusion on both the distribution and value of the wall stress. The inclusion of RS leads not only to a significant reduction in the maximum stress value, but also to a different location for the maximum stress areas. Therefore, the inclusion of RS is of great influence on AAA rupture prediction.

The proposed method is based on the hypothesis that the MPS has the same direction across the thickness of the wall. We tested this hypothesis on the analyzed cases and demonstrated that it holds for the

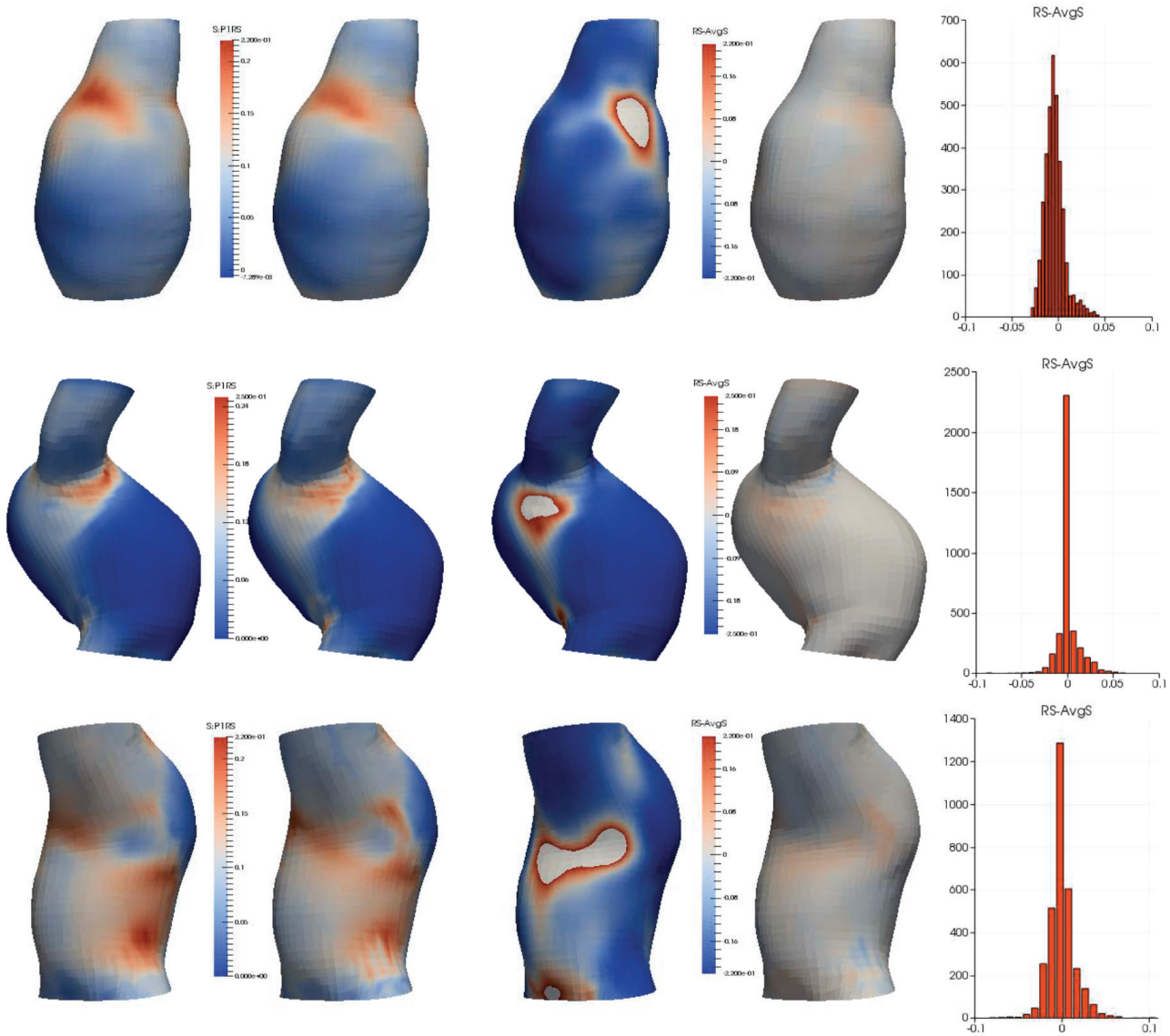

(a)

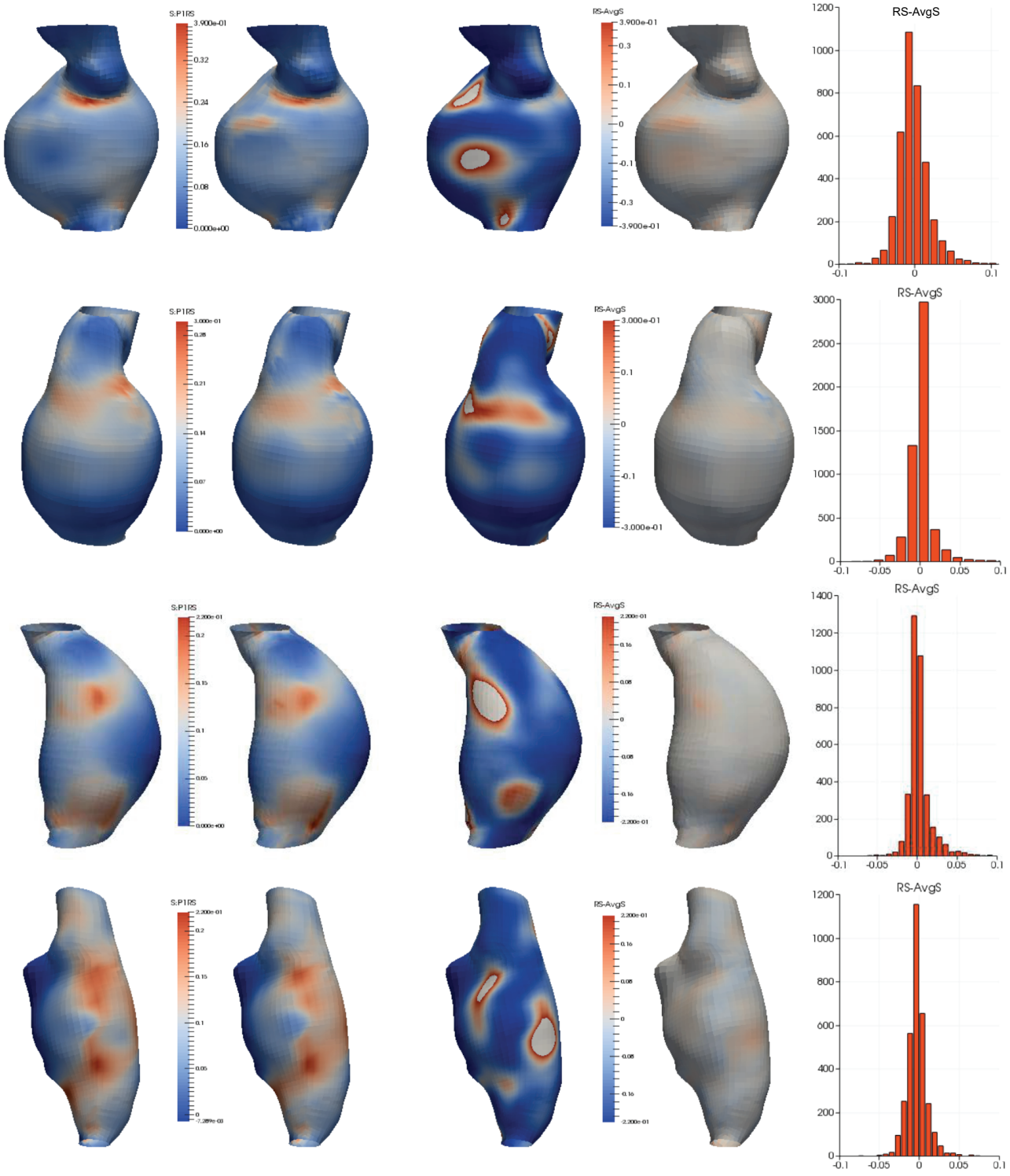

(b)

Fig. 6a, b. MPS distributions on the external arterial surface obtained using the new method for RS inclusion (column 1), the existing method for RS inclusion (column 2) and without RS inclusion (column 3) for seven AAA cases [MPa]. The first three columns share the same color scale. In column 3, the areas with stress higher than in the first two columns are marked in white. Column 4 presents the difference between stresses obtained using the new and the existing methods of RS inclusion, with a histogram of these differences presented in the last column

most part of the wall surface, even for complex geometries such as AAA.

While the proposed method is very fast in predicting the influence of RS on the MPS in the arterial wall, it has some limitations compared to other methods. Because it is based on averaging of MPS in the arterial wall, the new method does not actually compute the values of the RS or all the components of the wall stress. Therefore, it

does not provide a complete picture of the wall stress distribution under the influence of RS and cannot be used to perform simulations such as estimation of opening angle, artery inflation, or extraction of the unloaded geometry. Nevertheless, the method is very useful in applications where the maximum principal stress in the AAA wall is needed, such as the estimation of rupture potential index for an AAA, when coupled with a fast method for AAA stress evaluation procedure [15].

Acknowledgements

This work was partially funded by the 2016 Sheffield International Mobility Scheme, which is gratefully acknowledged. We wish to acknowledge the Raine Medical Research Foundation for funding G. R. Joldes through a Raine Priming Grant, and the Department of Health, Western Australia, for funding G. R. Joldes through a Merit Award.

References

[1] GASSER T.C., AUER M., LABRUTO F., SWEDENBORG J., ROY J., *Biomechanical rupture risk assessment of abdominal aortic aneurysms: Model complexity versus predictability of finite element simulations*, European Journal of Vascular and Endovascular Surgery, 2010, 40, 176–185, DOI: 10.1016/j.ejvs.2010.04.003.

[2] FILLINGER M.F., RAGHAVAN M.L., MARRA S.P., CRONENWETT J.L., KENNEDY F.E., *In vivo analysis of mechanical wall stress and abdominal aortic aneurysm rupture risk*, Journal of Vascular Surgery, 2002, 36, 589–597, DOI: 10.1067/mva.2002.125478.

[3] MARTUFI G., GASSER T.C., *Review: The Role of Biomechanical Modeling in the Rupture Risk Assessment for Abdominal Aortic Aneurysms*, Journal of Biomechanical Engineering, 2013, 135, 021010–021010–10, DOI: 10.1115/1.4023254.

[4] RACHEV A., GREENWALD S., *Residual strains in conduit arteries*, Journal of Biomechanics, 2003, 36, 661–670, DOI: 10.1016/S0021-9290(02)00444-X.

[5] CALLAGHAN F.M., LUECHINGER R., KURTCUOGLU V., SARIKAYA H., POULIKAKOS D., BAUMGARTNER R.W., *Wall stress of the cervical carotid artery in patients with carotid dissection: a case-control study*, American Journal of Physiology. Heart and Circulatory Physiology, 2011, 300, H1451–8, DOI: 10.1152/ajpheart.00871.2010.

[6] CHUONG C.J., FUNG Y.C., *On Residual Stresses in Arteries*, Journal of Biomechanical Engineering, 1986, 108, 189–192.

[7] TABER L.A., HUMPHREY J.D., *Stress-Modulated Growth, Residual Stress, and Vascular Heterogeneity*, Journal of Biomechanical Engineering, 2001, 123, 528–535, DOI: 10.1115/1.1412451.

[8] PEÑA J.A., MARTÍNEZ M.A., PEÑA E., *Layer-specific residual deformations and uniaxial and biaxial mechanical properties of thoracic porcine aorta*, Journal of the Mechanical Behavior of Biomedical Materials, 2015, 50, 55–69, DOI: 10.1016/j.jmbbm.2015.05.024.

[9] RAGHAVAN M.L., TRIVEDI S., NAGARAJ A., MCPHERSON D.D., CHANDRAN K.B., *Three-dimensional finite element analysis of residual stress in arteries*, Annals of Biomedical Engineering, 2004, 32, 257–263, DOI: 10.1023/B:ABME.0000012745.05794.32.

[10] BALZANI D., SCHRÖDER J., GROSS D., *Numerical simulation of residual stresses in arterial walls*, Computational Materials Science, 2007, 39, 117–123, DOI: 10.1016/j.commatsci.2005.11.014.

[11] HORNY L., ADAMEK T., GULTOVA E., ZITNY R., VESELY J., CHLUP H., KONVICKOVA S., *Correlations between age, prestrain, diameter and atherosclerosis in the male abdominal aorta*, Journal of the Mechanical Behavior of Biomedical Materials, 2011, 4, 2128–2132, DOI: 10.1016/j.jmbbm.2011.07.011.

[12] AMBROSI D., GUILLOU A., DI MARTINO E.S., *Stress-modulated remodeling of a non-homogeneous body*, Biomechanics and Modeling in Mechanobiology, 2008, 7, 63–76, DOI: 10.1007/s10237-007-0076-z.

[13] POLZER S., BURSA J., GASSER T.C., STAFFA R., VLACHOVSKY R., *A numerical implementation to predict residual strains from the homogeneous stress hypothesis with application to abdominal aortic aneurysms*, Annals of Biomedical Engineering, 2013, 41, 1516–1527, DOI: 10.1007/s10439-013-0749-y.

[14] SCHRÖDER J., VON HOEGEN M., *An engineering tool to estimate eigenstresses in three-dimensional patient-specific arteries*, Computer Methods in Applied Mechanics and Engineering, 2016, 306, 364–381, DOI: 10.1016/j.cma.2016.03.020.

[15] JOLDES G.R., MILLER K., WITTEK A., DOYLE B., *A simple, effective and clinically applicable method to compute abdominal aortic aneurysm wall stress*, Journal of the Mechanical Behavior of Biomedical Materials, 2016, 58, 139–148, DOI: 10.1016/j.jmbbm.2015.07.029.

[16] JOLDES G.R., MILLER K., WITTEK A., FORSYTHE R.O., NEWBY D.E., DOYLE B.J., *BioPARR: A software system for estimating the rupture potential index for abdominal aortic aneurysms*, Scientific Reports, 2017, 7, 4641, DOI: 10.1038/s41598-017-04699-1.

[17] FUNG Y.C., *What Are the Residual-Stresses Doing in Our Blood-Vessels*, Annals of Biomedical Engineering, 1991, 19, 237–249, DOI: 10.1007/bf02584301.

[18] LU X., ZHAO J.B., WANG G.R., GREGERSEN H., KASSAB G.S., *Remodeling of the zero-stress state of femoral arteries in response to flow overload*, American Journal of Physiology. Heart and Circulatory Physiology, 2001, 280, H1547–59.

[19] AUER M., GASSER T.C., *Reconstruction and Finite Element Mesh Generation of Abdominal Aortic Aneurysms From Computerized Tomography Angiography Data With Minimal User Interactions*, IEEE Transactions on Medical Imaging, 2010, 29, 1022–1028, DOI: 10.1109/TMI.2009.2039579.

[20] POLZER S., GASSER T.C., *Biomechanical rupture risk assessment of abdominal aortic aneurysms based on a novel probabilistic rupture risk index*, Journal of The Royal Society Interface, 2015, 12, 20150852, DOI: 10.1098/rsif.2015.0852.

[21] DE PUTTER S., WOLTERS B.J.B.M., RUTTEN M.C.M., BREEUWER M., GERRITSEN F.A., VAN DE VOSSE F.N., *Patient-specific initial wall stress in abdominal aortic aneurysms with a backward incremental method*, Journal of Biomechanics, 2007, 40, 1081–1090, DOI: 10.1016/j.jbiomech.2006.04.019.

[22] RIVEROS F., CHANDRA S., FINOL E.A., GASSER T.C., RODRIGUEZ J.F., *A pull-back algorithm to determine the unloaded vascular geometry in anisotropic hyperelastic AAA passive mechanics*, Annals of Biomedical Engineering, 2013, 41, 694–708, DOI: 10.1007/s10439-012-0712-3.